

LASER SURFACE MODIFICATION OF AISI 1025 STEEL

NIK NADIA FARHANA BT NIK ZULKIFLI

Report submitted in fulfillment of the requirements for the award of the degree of

Bachelor of Mechanical Engineering

Faculty of Mechanical Engineering

UNIVERSITI MALAYSIA PAHANG

JUNE 2013

ABSTRACT

Low carbon steels tends to fail due to high wear applications. This project focused on laser surface modification of AISI 1023 steel to improve surface hardness properties. In this project, Nd:YAG laser JK300HPS was used to modify the surface on substrate surface. Three set parameters which of laser power, pulse duration and overlap percentage were set as respective range of 1700 to 2500 W, 0.7 to 1.0 ms and 0 to 50%. The characterization for treated samples was conducted for hardness test and metallographic study. Hardness test were carried out by using Vickers indenter with $Hv_{0.1}$. Optical microscope was used to study the depth of treated sample for metallographic study. From the findings, lower speed produced higher hardness of 461 $Hv_{0.1}$. The hardness result that obtained from the study increased 300 % from the substrate region. The depth of modified layer ranged between 50 and 400 μm . These findings were important for structural material design.

ABSTRAK

Keluli karbon yang rendah cenderung untuk gagal kerana kerosakan tinggi berlaku pada aplikasi. Projek ini memberi tumpuan kepada pengubahsuaian permukaan laser AISI 1023 keluli untuk memperbaiki sifat-sifat kekerasan permukaan. Dalam projek ini, Nd: YAG laser JK300HPS digunakan untuk diubahsuai permukaan di atas permukaan substrat. Tiga parameter set yang kuasa laser, tempoh nadi dan pertindihan peratusan telah ditetapkan sebagai julat masing-masing 1700-2500 W, 0,7-1,0 ms dan 0 kepada 50%. Pencirian sampel yang di laser telah dijalankan untuk ujian kekerasan dan kajian metalografi. Kekerasan ujian telah dijalankan dengan menggunakan Vickers indenter dengan menggunakan $Hv_{0.1}$. Mikroskop optik telah digunakan untuk mengkaji ketebalan sampel yang di laser untuk kajian metalografi. Hasil penemuan ini mendapati, kelajuan yang lebih rendah yang dihasilkan kekerasan yang lebih tinggi iaitu 461 $Hv_{0.1}$. Hasil kekerasan yang diperolehi daripada kajian meningkat 300% dari kawasan substrat. Ketebalan lapisan diubahsuai adalah antara 50 dan 400 μm . Penemuan ini adalah penting bagi reka bentuk bahan struktur.

TABLE OF CONTENTS

	Page
TITLE PAGE	I
EXAMINERS DECLARATION	II
SUPERVISOR'S DECLARATION	III
STUDENT'S DECLARATION	IV
DEDICATION	V
ACKNOWLEDGEMENT	VI
ABSTRACT	VII
TRANSLATION OF ABSTRACT	VIII
TABLE OF CONTENTS	IX
LIST OF TABLES	XIII
LIST OF FIGURES	XIV
LIST OF ABBREVIATIONS	XVII
CHAPTER 1	
INTRODUCTION	1
1.1 Introduction	1
1.2 Objective	2
1.3 Problem Statement	2
1.4 Project Scope	2

CHAPTER 2	LITERATURE REVIEW	3
2.1	Introduction	3
2.2	Laser System	3
2.3	Laser Hardening	5
	2.5.1 Duty Cycle	7
	2.5.2 PRF	
	2.5.3 Power Measurement	8
2.4	Mild Steel	9
2.5	Parameter Effects on Surface Properties	10
	2.5.1 Hardness	
	2.5.2 Overlap	15
	2.5.3 Surface Roughness	18
	2.5.4 Microscopic Analysis	19
	2.5.5 Anova Analysis	20
CHAPTER 3	METHODOLOGY	22
3.1	Introduction	
3.2	Sample Preparation of AISI 1025	23
	3.2.1 Material	
	3.2.2 Cutting the Workpiece	
	3.2.4 Composition Test	31
3.3	Design of Experiment (DOE)	32

3.4	Laser Process	35
	3.4.1 Experiment Procedure	37
3.5	Characterization	
	3.5.1 Hardness Test	
	3.5.2 Microstructure Analysis	38
	3.5.3 Surface Roughness	40
CHAPTER 4	RESULT AND DISCUSSION	35
4.1	Microstructure Observation	35
	4.1.1 Optical Microscope	
4.2	Surface Roughness	40
4.3	Microstructural Analysis	41
	4.3.1 Depth	
4.4	Hardness Test	42
	4.4.1 Hardness across the Depth	
4.5	Anova Analysis	43
	4.5.1 Depth	45
	4.5.2 Hardness Properties	49
	4.5.3 Surface Roughness	51
	4.5.4 Optimization	55

CHAPTER 5	CONCLUSION	58
	5.1 Conclusion	
	5.2 Recommendation	
REFERENCES		59
APPENDIX		63

LIST OF TABLES

Table No.	Title	Page
2.1	Composition of mild steel	9
2.2	Analysis of variance (ANOVA) test for surface roughness, Ra.	21
3.1	Composition of mild steel	26
3.2	Variable parameters and experimental design levels	27
3.3	Laser Nd:YAG Performance	28
4.1	Design of Experiment for ANOVA analysis	44
4.2	ANOVA for depth analysis	45
4.3	ANOVA for hardness analysis	49
4.4	ANOVA for surface roughness analysis	52
4.5	Criteria of parameter that was chosen	56
4.6	Solution for optimisation	57

LIST OF FIGURES

Figure No.	Title	Page
2.1	Schematic of Nd:YAG Laser	4
2.2	RF Pulse Train	8
2.3	Schematic diagram of a laser surface hardening process	9
2.4	Micro hardness profile by using vickers and rockwell hardness test	10
2.5	Microhardness vs distance surface laser hardening with heating and cooling rates, after 1,3 and 27 samples	11
2.6	Profile of the relationship between the micro-hardness of HAZ	13
2.7	Hardness profile along the depth of the laser transformation-hardened layer.	14
2.8	Schematic diagram of laser power pulse trains and their corresponding partially overlapping spot	17
2.9	Metallograph of HAZ induced by pulsed Nd:YAG laser forming with different overlapping rate P_{PER} .	15
2.10	SEM micrograph of the cross sections.	16
2.11	The Schematic diagrams showing sample preparation for cross-section microstructure observations on laser hardened zones.	20
3.1	Flow Chart of Methodology	23
3.2	Flow chart for sample preparation	24
3.3	Raw material of specimen	25
3.4	EDM machine	
3.5	Spark Emission Spectrometer	26
3.6	Experimental design module selection	27

3.7	Experiment types selection	28
3.8	The design of experiment of laser surface processing of AISI 1025 steel	29
3.9	Laser system setup	30
3.10	Setting for CNC board	31
3.11	Vickers Rockwell Component	32
3.12	Grinding process	33
3.13	Specimen after grinding process	
3.14	Polish clothes and grades	
3.15	Perthometer	34
4.1	Surface morphology of laser modified AISI 1025 at constant PRF of 60 Hz, three different Speed and Energy at of (a),(d),(g) 1.7 J, (b),(e),(h) 2.0 J and (c),(f),(i) 2.5 J.	37
4.2	Surface morphology of laser modified AISI 1025 at constant PRF of 50 Hz, three different Speed and Energy at of (a),(d),(g) 1.7 J, (b),(e),(h) 2.0 J and (c),(f),(i) 2.5 J.	38
4.3	Surface morphology of laser modified AISI 1025 at constant PRF of 40 Hz, three different Speed and Energy at of (a),(d),(g) 1.7 J, (b),(e),(h) 2.0 J and (c),(f),(i) 2.5 J.	39
4.4	The Graph Shows the Surface Roughness And Samples Reading	40
4.5	The Depth	41
4.6	Vicker's Rockwell Hardness Test Graph	42
4.7	Hardness across the depth	43
4.8	Depth of modified layer at variations of Speed and Peak Power at constant PRF 40 Hz	46
4.9	Depth of modified layer at variations of Speed and Peak power at constant PRF 60 Hz	47

4.10	Depth of modified layer with changes of PRF versus Peak Power and constant speed of 1800 mm/min.	
4.11	Depth of modified layer at variations of PRF and speed at constant peak power 1700 W	48
4.12	Depth of modified layer at variations of PRF versus speed with constant peak power of 2500 W	
4.13	Hardness of laser modified AISI 1025 responding to Speed and Peak power at constant PRF 40 Hz	50
4.14	Hardness of laser modified AISI 1025 responding to PRF and Peak power with constant speed of 1800 mm/min.	51
4.15	Hardness of laser modified AISI 1025 responding to PRF and Speed with constant of Peak Power at 2500 W	
4.16	Surface roughness of laser modified AISI 1025 responding to Speed and Peak power at constant PRF 40 Hz	53
4.17	Surface roughness of laser modified AISI 1025 responding to Speed and Peak power at constant PRF 60 Hz	
4.18	Surface roughness of laser modified AISI 1025 responding to PRF and Peak power with constant at speed 1400 mm/min	54
4.19	Surface roughness of laser modified AISI 1025 responding to PRF and Speed with Peak power at 1700 W	55
4.20	Surface roughness of laser modified AISI 1025 responding to PRF and Speed with Peak power at 2500 W	

LIST OF ABBREVIATIONS

P _p	Peak Power
P _{ave}	Average Power
O _f	Overlap factor
I	Irradiance
HAZ	Heat Affected Zone
P _{PER}	Overlap rate
Nd:YAG	Neodymium-Doped Yttrium Aluminum Garnet
AISI	American Iron and Steel Institute
C	Carbon
Mn	Manganese
Si	Silicom
Cr	Chromium
Ni	Nitrium
Mo	Molybdenum
V	Vanadium
Cu	Cuprum
P	Phosphorus
S	Sulfur
Fe	Ferum
HV	Hardness Vicker's

CHAPTER 1

INTRODUCTION

1.1 PROJECT BACKGROUND

Lasers have been used in a number of ways to increase the wear resistance and durability of the surface for metal. Recently, automobile and machine tool industries pay attention to the technology of laser surface hardening due to a short hardening time, a small deformation after hardening, an ease of automation, and a selective hardening of part according to the function of part. Janez et al. researched into the influence of process parameters of laser surface melt hardening on residual stresses in thin plate. Selvan and Subramanian researched into the effect of process parameters and an absorption coating of laser surface hardening on the hardness and the microstructure changes of structural steel.

Laser heat treating is the most common process in the group of surface modification techniques that include alloying, glazing, and cladding. "Heat treating" could imply a number of processes common to metallurgical practice. This project will focus on the transformation hardening process using lasers to produce changes in surface properties.

Heat treating produced the light by a laser is an industrial tool. Light is directed to the work piece using optics, which causes materials to heat, melt, or vaporize. This type of surface treatment is used for improvement of hardness by changing the structure and improvement of the abrasion wear resistance, mostly by laser treatment.

1.2 PROBLEM STATEMENT

Recently, laser surface modification has been applied to improve the properties of the near surface region, which can determine the performance of a material. Laser surface modification is a fast and efficient technique for producing surface layers with improved properties. Material like AISI 1025 has been widely used in tool steel industry however the crack and premature failure is still happened. Thus, tool steel industry required the technology of laser surface modification due to short time processing and high production compare to conventional method.

1.3 PROJECT OBJECTIVE

The objectives of this study are:

- i. Study of laser hardening properties as well as mild steel.

1.4 SCOPE OF THE PROJECT

The scopes of this study include

- i. Material was used AISI 1025
- ii. Laser harden steel samples using full factorial Design of experiment.
- iii. Characterise as received and laser hardened sample for Metallographic study and Micro-hardness properties
- iv. Optimized the processing parameters for minimum surface roughness and maximum properties

CHAPTER 2

LITERATURE REVIEW

2.1 INTRODUCTION

The hardening of steel was conducted by heating up a work piece to near its melting temperature then quickly quenching it. This heat treatment process causes significant changes in the microstructure of the steel which directly corresponds to its metallic properties. The martensitic structure that is formed is responsible for the increased material hardness. The main methods of hardening are flame, induction, and laser hardening. Laser hardening is especially attractive for surface hardening of complicated shapes or large objects because it allows for absolute control on the surface hardness and texture.

2.2 LASER SYSTEM

The Nd: YAG laser is the most common type of solid-state lasers are used in a variety of fields at this moment because of its great thermal and mechanical properties and easy maintenance (W. Koechner and et al., 1995). In the study of laser processing method recently, pulsed Nd: YAG laser has many advantages over the commonly used CO₂ laser has been investigated vigorously. It may focus on short-wave point smaller than the CO₂ laser. Moreover, the processing of materials, suitable laser power density needed for a particular process and laser power density can be controlled by the current pulse width and pulse repetition rate, known as the major factor for the a particular properties of materials (M.W. Timothy et al., 1987)

Nd: YAG laser is one of the solid state laser. Suspended solids using laser ion in the crystal matrix to produce laser light. Ions or dopants provide electrons for excitation, while the crystalline matrix of ion energy travels. The two major classes of dopants in laser medium is Chromium (Cr^{3+}) to the ruby laser and Neodinium (Nd^{3+}) to Nd: YAG and Nd: glass laser. Nd: YAG and Nd: glass lasers are generally very similar to each other in structure and lasing action. Excitation accomplished with krypton or xenon flash lamp, and output wave near infrared spectral region is obtained. Nd: glass laser glass host materials for neodymium ions. Glass rods have the benefit that they can grow to larger sizes is more economical than YAG crystal, but glass has a lower thermal conductivity that limits the operation of this pulsed Nd: glass laser. Thus, the Nd: glass laser used in applications requiring a lower pulse repetition rate and higher pulse energy more than 100 Joules per pulse. Generally, the operation of the laser pulse Nd makes them appropriate for piercing holes in keyhole welding applications.

The host material in Nd: YAG lasers is a complex crystal of Yttrium-Aluminum-Garnet (YAG) with the chemical composition $\text{Y}_3\text{Al}_5\text{O}_{12}$. The YAG crystal has a relatively high thermal conductivity, which improves thermal dissipation in the laser cavity, so continuous wave operation up to a few hundred Watts is possible.

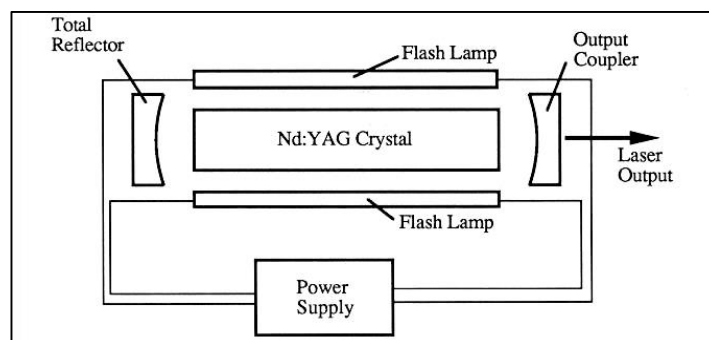


Figure 2.1: Schematic of Nd:YAG Laser

Source: W. Koechner and et al. (1995)

The Nd:YAG lasers use several long pulses to ignite the fuel, producing faster and more uniform ignition. The researchers say that such igniters could produce better performance and fuel economy and less harmful emissions. (Anthony E. 1986). Furthermore, it is widely used in wide range of applications such as micromachining, holography, range finding, medical surgery, material processing, etc. (G. Liedl et al., 1996).

In medical surgery, ND: YAG laser used in ophthalmology to correct posterior capsular opacification, a condition that may occur after cataract surgery, and peripheral iridology in patients with acute angle-closure glaucoma, where it has replaced surgical iridectomy. Frequency doubled Nd: YAG laser in certain wavelength was used for pan-retinal photocoagulation in patients with diabetic retinopathy. It is also help to remove various types of cancer at complicated area and more effectiveness. (Brent. 2010)

Nd: YAG laser is also used in manufacturing of engraving, etching, or marking a variety of metals and plastics. They are widely used in the manufacture of cutting and welding steel, semiconductors and a variety of alloys. For automotive applications that cut and weld steel at a certain power level. Nd: YAG laser is also used to make a mark on the surface of transparent materials such as glass or acrylic glass. Up to 400 W laser is used for selective laser melting of metal in the manufacture of an extra layers. In aerospace usage, they can be used to drill holes for the cooling air flow enhanced exhaust efficiency. (Walter. 1988)

2.3 LASER HARDENING

Laser transformation hardening is a process in which the phase changes due to irradiation of steel component surfaces with a laser beam. The surface area is heated to a temperature exceeding the transformation temperature lead to austenitization. Surrounding material acts as an efficient heat sink. Heat is transferred by conduction from the surface, inducing rapid cooling. Austenitized material, provided with adequate quantity of carbon, formed martensite when quenching, producing a hard and wear resistant surface. Longer interaction time allows more heat to be conducted into

the matter prior to the melting temperature reached at the surface, resulting in a deeper layer of hard. Higher traverse and power density results in quicker cooling rate, at the expense of the hard layer depth. (P.Henrikki. 2007)

Figure 2.2 shows the surface layer is heated above its austenite transformation temperature, but below the melting temperature by high-power laser beam energy (up to 4 kW in previous study) traveling along a specified direction (H.G. Woo. 1998). As a result, earlier microstructure consisting of ferrite and pearlite transformed into austenite phase. At this higher temperature, substrate material microstructure homogenized by diffusion of carbon. Once heated, the material is quickly cooled, causing the hard martensite phase due to the rapid heat conduction from the surface into the bulk substrate material. Taking into consideration temperature distribution around point A shown in Figure 2.2, the surface temperature along the laser travel direction rapid increase in the laser area and then suddenly dropped laser irradiation area.

The form surface temperature distribution across the laser travel direction is the same as the general Gaussian function. The highest temperature at the centre point while it decreases the even further from the point A. In terms of depth, the temperature dropped very steeply because of the large heat conduction into the bulk material. With this temperature distribution, only a small portion on the heated surface temperature of austenite and martensite transformed into a hard layer. For this case, because the surface hardening is based on metal transformation in response to heated by the laser beam energy, surface hardening is often referred to as laser surface transformation hardening.

As compared with CO₂ lasers, Nd:YAG lasers have a shorter wavelength and thus normally do not need to coat the surface that is to be treated. Such lasers are more easily controllable and can be delivered to component surfaces by fibre optics and are therefore more suited for laser transformation hardening than the CO₂ lasers. However, very limited data is available on the appropriate selection of processing parameters to achieve optimal results. As cited, Wu et al. numerically simulated the effects of laser spatial and temporal intensity distributions on laser transformation

hardening (hardening depth and connectivity of hardened zones between adjacent hardening spots) using a pulsed laser and indicated that temporal pulse shape has great effects on hardening results. Woodard and Dryden provided analytical solutions for discrete/spot laser surface transformation hardening, including the variation of diameter and depth of hardening zones. No information is available for the determination of processing conditions during discrete laser transformation hardening using a pulsed laser. In J. Jiang studied, discrete laser spot hardening of AISI O1 tool steel has been studied using a pulsed Nd:YAG laser. Effect of various laser processing parameters, including laser pulse energy, pulse duration and defocus distance, on characteristics of the laser treated spots are investigated.

2.3.1 Duty Cycle

Duty cycle or duty factor used to measure the fraction time radar is transmitting. It is vital to relates between peak and average power for total energy output. It is also effect the strength of the reflected signal as well as the required power supply capacity.

2.3.2 PRF

For PRF the most radio frequency (RF) measurements are either continuous wave or pulsed RF. Continuous wave RF is uninterrupted RF as the oscillator. The amplitude modulated (AM), frequency modulated (FM), and phase modulated RF considered CW since the RF continues to be present. Power can alter with time resulting modulation period, but in the meantime the presence of RF is for clarity and simpler, all the RF pulse is considered to have similar amplitude. Pulses at a regular time to arrive at the rate according to the frequency of pulse repetition frequency (PRF) so many pulse per second. Pulse repetition interval (PRI) and PRF is the reciprocal of each other. The formula to calculate the PRF is shown in equation (2.1).

$$PRF = \frac{1}{T} = \frac{1}{PRI} \quad (2.1)$$

2.3.3 Power Measurement

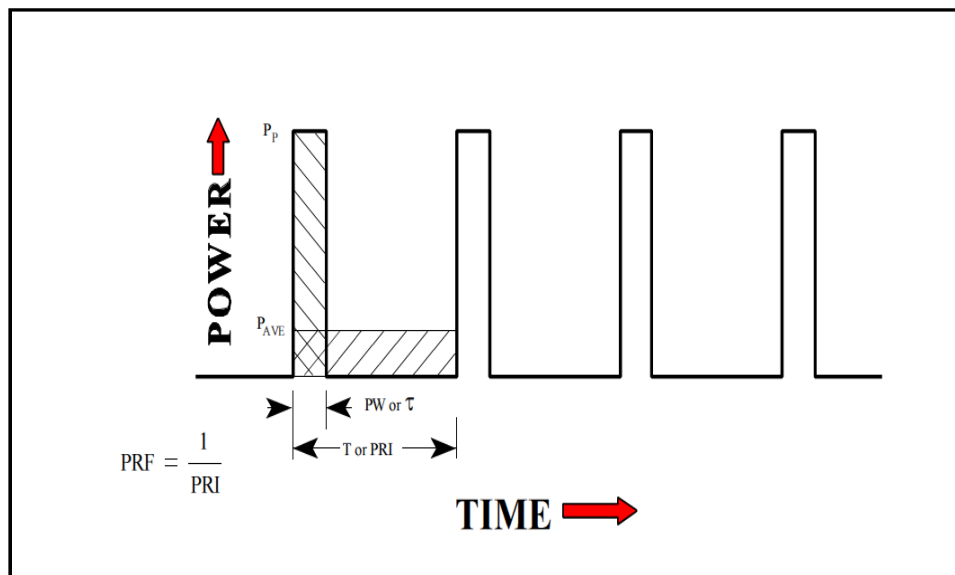


Figure 2.2: RF Pulse Train

Power measurements classified as either a pulse peak power, P_p , or average power, P_{ave} . The actual power of the RF pulse happen during the pulses, but the measurement method to measure the heating effect of RF energy to get the average power. Value is used when it is in line to be a reference. Frequently, it is need to convert from P_p and P_{ave} . The equation below (2.2) and (2.3) shows a comparison between P_p and P_{ave} .

Since the two values are equal:

$$P_{ave} \times T = P_p \times PW \quad (2.2)$$

$$P_{ave}/P_p = PW/T \quad (2.3)$$

Using equation (2.1)

$$P_{ave}/P_p = PW/T = PW \times PRF = PW/PRI = \text{duty cycle.}$$

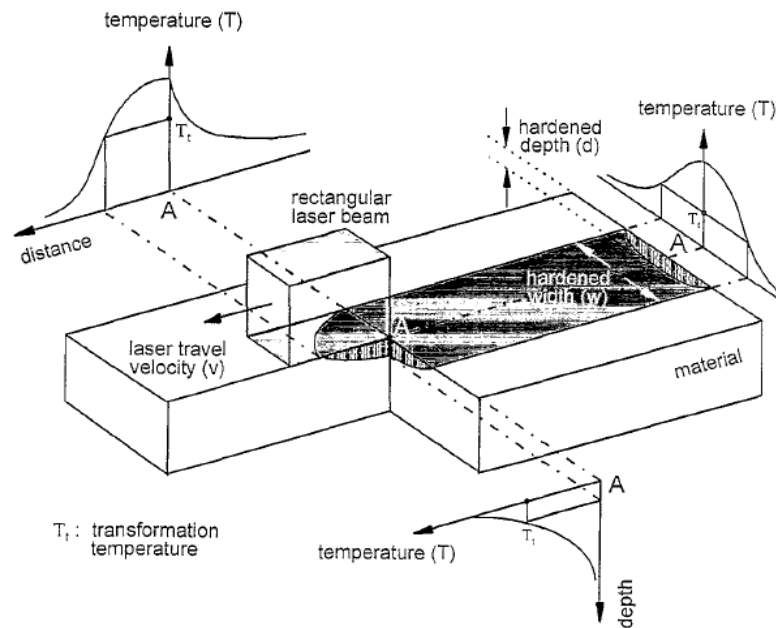


Figure 2.3: Schematic diagram of a laser surface hardening process

Source: H.G. Woo. (1998)

2.4 MILD STEEL

Table 2.1 shows the Chemical composition of AISI 1025 steel that was analysed using OXFORD INSTRUMENT Foundry-Master spectroscopy. It shows the percent of carbon content is lower. The carbon composition can affect the austenite stabilizer, strengthens martensite, and determines the phase distribution.

Table 2.1: Composition of mild steel

Element	C	P	Mn	Si	S	Ni
Mass (%)	0.155	0.016	0.660	0.140	0.012	0.026
	Cr	Cu	Al	Ti	Mo	Nb
	0.014	0.007	0.031	<0.003	0.002	0.001

Source: Vives (2008)

2.5 PARAMETER EFFECTS ON SURFACE PROPERTIES

2.5.1 Hardness

Figure 2.4 shows the micro hardness profile by using Vickers and Rockwell Hardness Test at constant power which is 500 W. In this study, the hardness near the surface is very high. The hardness reading quite constant till it drops after a certain distance from it surface.

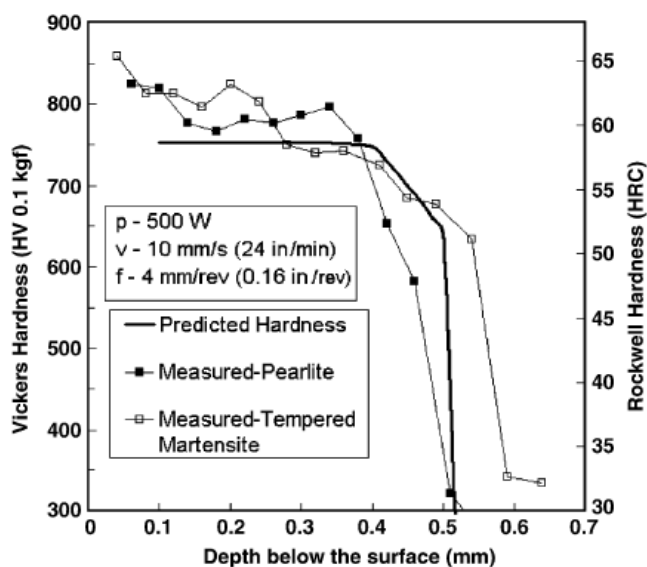


Figure 2.4: Micro Hardness Profile by Using Vickers And Rockwell Hardness Test

Source: Stephen (2006)

Figure 2.5 shows that the overview of micro hardness after undergoes laser hardening with heating and cooling rates. The depth s of hardening is depend on number of cycle, when the number of cycle less than 3, it will increase, but then remain constant for high number of cycles. It assumed that increasing time for heat impact the temperature and makes the larger depths and become stationary for high irradiation time. It determined the limit of the zone depth and the depth of hardening also. The

microstructures result is in the region between the hardened and transient zone after laser hardening.

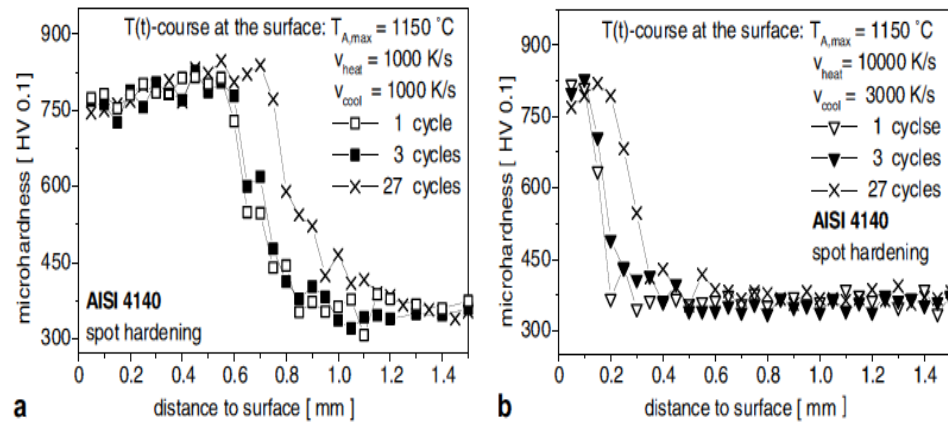


Figure 2.5: (a) Microhardness versus distance surface laser hardening with heating and cooling rates. (b) After 1,3 and 27 samples

Source: Mioković (2007)

Figure 2.6 shows the micro-hardness of HAZ with different P_{PER} at different position of the irradiated zone by pulsed Nd:YAG laser forming. The micro-hardness is increasing in comparison to the matrix material, and the micro-hardness increases with the P_{PER} increasing, and the hardness in the upper layer and the center of the laser beam is more than other regions. From the upper surface to the bottom surface and from the laser beam center to outer, the micro-hardness is decreasing, as shown in Figure 3 (a) and (b). As shown in Figure 3 (c)–(h), the influence of laser power, the pulse energy, the pulse width, the pulse rate, the scanning velocity and the scanning numbers on the hardness of stainless steel 1Cr18Ni9 in the same region of the samples are illustrated. From which it can be seen that the difference in hardness varies between 180 and 250 N/mm² (Hv₁₀₀), which have the meaning that the micro-hardness of irradiated zones is increasing in comparison to 150 N/mm²(Hv₁₀₀) of the matrix materials.

The micro-hardness initially increases with the laser power, pulse energy and pulse width and begins to decrease at a certain parameters, as there is a certain

parameters resulting in a maximum micro-hardness for a certain material and processing parameters. The micro-hardness decreases with higher of pulse rate, and increases approximately linearly as the scanning velocity increasing in a given conditions. The micro-hardness decreases as the scanning numbers increases and begins to increase at a certain processing parameters, and the maximum micro-hardness is acquired when the sheet scanned one time. This means that the work hardening is not a constant in all parts of the specimen, it differs depending on the laser parameters. The micro-hardness of the irradiated region is bigger than the raw material, by reason of that the grains after laser irradiated become smaller and closer compared with raw materials under the action of the temperature gradient.

In the pulsed laser forming, the overlapping spot is the most influential factors for the interactive time and energy. When scanning speed is in the scale of the overlapping, the overlapping rate is the main influential factor for laser forming.

The microstructure in the irradiated zones by pulsed Nd:YAG laser forming is layered when the overlapping rate is not zero, the case hardening of the HAZ is layered and inhomogeneous in the laser scanning line, and the metallograph in the different location in the scanning line is varied.